Rotational energy dispersions for van der Waals molecular clusters: Analytic descriptions for Rg_3, Rg_4, and Rg_6

Lawrence L. Lohr [a] and Carl H. Huben
Department of Chemistry, University of Michigan, Ann Arbor, Michigan 48109-1055

(Received 9 April 1993; accepted 12 July 1993)

We have obtained analytic expressions, parametric in centrifugal displacement coordinates, which provide exact classical descriptions of the rotational energy dispersions, that is, the dependence of the combined rotational and "electronic" (vibrational potential) energies on the rotational angular momenta, for small molecular clusters bound by van der Waals interactions modeled by pairwise additive Lennard-Jones 6–12 potential energies. The clusters considered consist of three (equilateral triangle), four (tetrahedron), and six (octahedron) units and serve as models for small clusters of rare-gas atoms such as argon. This work represents an extension of our recently published study of analytic rotational energy dispersions for diatomic molecules bound by harmonic oscillator, Morse, or Lennard-Jones potentials [J. Mol. Spectrosc. **155**, 205 (1992)]. A parallel set of studies were made using an angular momentum-conserving simulation program. The physical properties of the clusters that are addressed using our results include calculation of quartic and higher-order spectroscopic constants, location of rotational instabilities, and characterization of the "cubic" anisotropies for the spherical top clusters A_4 and A_6. Of particular interest is the result that for each of these cluster types the preferred direction of the rotational angular momentum is parallel to a molecular fourfold axis, leading to reduced symmetries of D_{2d} for tetrahedral A_4 and D_{4h} for octahedral A_6.

I. INTRODUCTION

The distortion of a rotating molecule from its equilibrium geometry and its effect upon the rotational energy levels has been recognized for a long time by molecular spectroscopists. Interest in these centrifugal effects, as they are often called, has increased in recent years due to the development of high-resolution spectroscopic techniques and to major advances in the theoretical description of highly excited rotational states of molecules. In a series of studies[1–6] we presented a new approach to centrifugal distortions and their associated rotational energy stabilizations which exploits *ab initio* electronic structure computational methods. This approach is direct, bypassing in its simplest applications the explicit calculation of spectroscopic constants such as vibrational frequencies as this information is implicitly contained in the *ab initio* electronic energy hypersurface. Specifically the method is particularly useful at any computational level for which analytic gradients of potential-energy hypersurface is available. Results were presented in our first study[1] for H_2^+, NH_3, CH_4, BF_3, and SF_6. More detailed studies followed[2–4] for H_2O, O_3, and PH_3, as well as an outline of a generalized extension of the method.[5] The procedure is structurally oriented, that is, it focuses on the question of the size and shape of molecules with nonzero rotational angular momentum. Centrifugal distortion spectroscopic constants are a very useful form of our computational output, providing an important and indispensable basis for comparison to experimental observations, yet their computation is in a way secondary to the main task. Stated differently, our studies are an exploration of molecular energy in those regions of nuclear-coordinate hyperspace which are accessible by centrifugal distortions from the equilibrium geometry.

In the most recent of our studies[6] we confined our attention to diatomic molecules as modeled by harmonic oscillator (HO), Morse oscillator (MO), and Lennard-Jones oscillator (LJO) potential energy functions. We obtained closed-form analytic expressions, parametric in the centrifugal displacement, for the dependence of the classical rotational energy upon the rotational energy momentum, that is, the rotational energy dispersion for each of these three model potentials. Further, through power-series reversions of the angular momentum as a function of displacement we obtained Padé approximants for the rotational energy dispersions which approximate well the exact parametric solutions and which may be used for fitting experimental spectroscopic data as they do not display the high angular momentum divergences associated with traditional power series representations of the energy. A particularly interesting result for the diatomic LJO is that the maximum stable centrifugal displacement is only $(5/2)^{1/6}-1=0.164\,99$ in units of the equilibrium separation for the nonrotating molecule; larger separations lead spontaneously to dissociation.

In our present study we obtain and characterize analytic descriptions of the rotational energy dispersions for deformable molecules. Specifically we expand the previous study[6] of the Lennard-Jones (LJO) diatomic to include larger clusters formed from atoms (or molecules) bound together by pairwise-additive LJO interactions. Such systems serve as excellent models for real clusters formed from rare-gas atoms or other closed-shell moieties. Indeed there have been many studies in recent years[7–21] describing the structures, stabilities, and dynamics, both rotational and vibrational, of such clusters with a particular focus on

[a] Author to whom correspondence should be addressed.

 0021-9606/93/99(9)/6369/9/$6.00

those formed from the rare-gas argon (Ar). Perhaps the closest in style to our present study is that of Li and Jellinek,[13] who used a simulation program to explore the distortion, isomerization, and fragmentation of the cluster Ar_{13}. Our study is focused on the smaller clusters A_3, A_4, and A_6, where A is an unspecified "particle" having LJO interactions, with most of the results being obtained and characterized analytically. We have complemented our analytic studies with the use an angular momentum-conserving simulation procedure closely related to that employed by Li and Jellinek;[13] our simulation results serve in part as a check on the correctness of the analytically obtained results.

We finally note that our work may be viewed as closely related to many of the studies[22–27] of centrifugal barriers in polyatomic systems and their role in fragmentation and scattering phenomena.

II. OUTLINE OF PROCEDURE

For a polyatomic molecule we consider the total electronic energy E_{el} (within the Born–Oppenheimer approximation) as a function of a set of internal nuclear coordinates $\mathbf{Q}=\{Q_i\}$, that is,

$$E_{el}=E_{el}(Q_1Q_2Q_3\cdots Q_n)=E_{el}(\mathbf{Q}). \tag{1}$$

The energy of rotation about the center of mass may be expressed classically in terms of these same coordinates via the moment of inertia tensor $\mathbf{I}(\mathbf{Q})$ and the rotational angular momentum $\mathbf{J}$, where $\mathbf{J}=\mathbf{I}\omega$, with ω being the angular velocity, as

$$E_{rot}=E_{rot}(\mathbf{Q},\mathbf{J})=(1/2)\mathbf{J}_t\mathbf{I}^{-1}\mathbf{J}, \tag{2}$$

where $\mathbf{I}^{-1}$ is the inverse of the matrix $\mathbf{I}$ and $\mathbf{J}_t$ is the transpose of the vector $\mathbf{J}$.

Thus the effective "potential" energy governing the motion of the nuclei is given by the $\mathbf{J}$-dependent sum of E_{el} and E_{rot}, that is, by

$$E_{eff}(\mathbf{Q},\mathbf{J})=E_{el}(\mathbf{Q})+E_{rot}(\mathbf{Q},\mathbf{J}), \tag{3}$$

where the $\mathbf{Q}$ dependence of E_{rot} and thus of E_{eff} is via the moment of inertia tensor $\mathbf{I}(\mathbf{Q})$.

For a number of purposes we seek extrema in nuclear coordinate space $\mathbf{Q}=\{Q_i\}$ of the effective energy E_{eff}. One important purpose is to find the rotational energy dispersion $E_{eff}(\mathbf{J})$ corresponding to the set of minima which classically are continuous with respect to both the magnitude and direction of $\mathbf{J}$ in the molecular frame. For such extrema of E_{eff}, not only do we require that $\nabla(E_{eff})=0$, but also that the hessian (second-derivative) matrix have positive eigenvalues. For small displacements from the zero angular momentum equilibrium structures the latter condition is assumed without demonstration to be satisfied. We do discuss, however, the important topic of symmetry breaking at sufficiently high angular momenta. In many cases the rotational energy will depend on only a subset, say m in number, of the total number, say n, of nuclear coordinates $\{Q_i\}$. In such cases there will be for a given $\mathbf{J}$ m equations of the type $\nabla_i(E_{el}+E_{rot})=0$ and $(n-m)$ of the type $\nabla_i E_{el}=0$. These conditions define in principle a centrifugal distortion pathway $\mathbf{Q}(\mathbf{J})$, although typically we cannot obtain it analytically and thus cannot obtain the desired rotational energy dispersion $E_{eff}(\mathbf{J})$ analytically. However expressing the pathway as $\mathbf{J}(\mathbf{Q})$ and substituting in $E_{eff}(\mathbf{Q},\mathbf{J})$ yields $E_{eff}(\mathbf{Q})$, which together with $\mathbf{J}(\mathbf{Q})$ defines the dispersion parametrically. Thus in many cases we can represent the dispersion $E_{eff}(\mathbf{J})$ by the pair of analytic relationships $E_{eff}(\mathbf{Q})$ and $\mathbf{J}(\mathbf{Q})$. In the remainder of this paper we present such analytic parametric rotational energy dispersions for van der Waals molecular clusters and show how they may be used to extract higher-order (quartic and above) spectroscopic constants.

III. THE LENNARD-JONES (6–12) POTENTIAL AND VAN DER WAALS CLUSTERS

The molecular systems whose rotational energy dispersions we wish to characterize are the weakly bound clusters of closed-shell molecules known as van der Waals clusters. Typical examples include clusters of rare-gas atoms or clusters of such molecules as carbon dioxide CO_2 or sulfur hexafluoride SF_6. Such clusters, and particularly those comprised of rare-gas atoms, are often modeled by a total electronic energy $E_{el}(\mathbf{Q})$ taken as a sum of pairwise-additive Lennard-Jones (6–12) oscillator (LJO) potential energy terms, where each term is of the form

$$V(r)=4d[(\sigma/r)^{12}-(\sigma/r)^6]. \tag{4}$$

In the above d is the well depth and σ is the "collision diameter." The equilibrium separation r_e is given by $2^{1/6}\sigma$. For purposes of this study we find it convenient to rewrite Eq. (4) by defining a reduced displacement $x=(r-r_e)/r_e$ and a new variable $z=1/(1+x)^2=(r_e/r)^2$, and by adding d to the energy, giving

$$V(z)=d(1-z^3)^2. \tag{5}$$

Further, dividing by d yields the dimensionless reduced form

$$v(z)=V(z)/d=(1-z^3)^2. \tag{6}$$

This form resembles that for the harmonic (Hooke's Law) oscillator, but with the potential energy being proportional to the square of a function of the displacement instead of to the square of the displacement itself. Further, as will be shown, many analytic relationships for pairwise-additive LJO systems have the form of polynomials in the displacement-related parameter z.

While most of our results will be presented and discussed for the dimensionless reduced form [Eq. (6)] for the LJO potential energy, thus making them applicable to any LJO clusters made up of identical moieties, we do present some numerical results for one very important class of examples, namely van der Waals clusters of argon (Ar) atoms. The parameters we have selected for the reference diatomic Ar_2 are the same as those used by Leitner, Whitnell, and Berry[12] in their study of the cluster Ar_3, namely $\sigma=3.40$ Å, corresponding to $r_e=3.82$ Å, and $d=84.1$ cm^{-1}. Other sets of Ar_2 parameters have also been pro-

TABLE I. Energy–angular momentum expressions parametric in displacements for LJO clusters.

Species	Direction	$\beta J^2[z^2(1-z^3)]$[a,b]	$\epsilon[(1-z^3)(5z^3+1)]$[c]
A_2	$\mathbf{J}\perp C_\infty$	6[d]	1[d]
$A_3(D_{3h})$	$\mathbf{J}\parallel C_3$	36	3
	$\mathbf{J}\parallel C_2$	6	1
$A_4(T_d)$	$\mathbf{J}\parallel S_4$	24	2
	$\mathbf{J}\parallel C_3$	36	3
$A_6(O_h$-*cis* only)	$\mathbf{J}\parallel C_4$	96	4
	$\mathbf{J}\parallel C_3$	144	6

[a] $z=1/(1+x)^2=(r_e/r)^2$.
[b] $\beta=B_e(A_2)/D_e(A_2)$, where $D_e(A_2)$ = well depth d.
[c] $\epsilon=E_{\rm eff}(Q)/D_e(A_2)$.
[d] The tabulated integers are multipliers of the expressions at the head of each column.

posed or used.[28–32] For the isotopic species $^{40}Ar_2$ the rigid-rotor constant $B_e=\hbar^2/2\mu r_e^2=0.058\ \text{cm}^{-1}$, where $\hbar$ is Planck's constant h divided by 2π and μ is the reduced mass $m(^{40}\text{Ar})/2$, so that the dimensionless reduced rigid-rotor constant $\beta=B_e/d=6.878\times10^{-4}$.

IV. ANALYTIC ROTATIONAL ENERGY DISPERSIONS

In Table I we present analytic rotational energy dispersion relationships parametric in centrifugal displacements for a number of simple cases, namely for the LJO clusters A_2, A_3 ($\mathbf{J}\parallel C_3$ and $\mathbf{J}\parallel C_2$), A_4 ($\mathbf{J}\parallel S_4$ and $\mathbf{J}\parallel C_3$), and A_6 ($\mathbf{J}\parallel C_4$ and $\mathbf{J}\parallel C_3$), with the expressions for A_6 being for the simplified model neglecting the three *trans* interactions. The corresponding structures may be described as follows: For A_3 with $\mathbf{J}\parallel C_3$ the structure is an expanded equilateral triangle (D_{3h}), but for $\mathbf{J}\parallel C_2$ it is an obtuse isosceles triangle (C_{2v}); for A_4 with $\mathbf{J}\parallel S_4$ the structure has two edges $\perp$ **J** which are extended, forming a flattened tetrahedron (D_{2d}) which approaches a square-planar structure (D_{4h}) for large displacements, while for $\mathbf{J}\parallel C_3$ the structure is a trigonal pyramid (C_{3v}) with an expanded triangular base; and for A_6 with $\mathbf{J}\parallel C_4$ the structure is a tetragonal bipyramid compressed in height and expanded in its equatorial plane (D_{4h}), but for $\mathbf{J}\parallel C_3$ the structure is a trigonally flattened octahedron (D_{3d}). For simplicity of notation we denote the dimensionless reduced effective energy $E_{\rm eff}(\mathbf{Q})/d=\epsilon_{\rm eff}(\mathbf{Q})$ as "ϵ," with no subscript. In each case the expressions in Table I are in terms of a single structural parameter $z=(1+x)^{-2}$, where x is the reduced displacement, with the tabulation giving the integer coefficients a and b which multiply the basic expressions. That is, for these simple cases we find

$$\beta J^2=a[z^2(1-z^3)], \tag{7}$$

$$\epsilon=b[(1-z^3)(5z^3+1)]. \tag{8}$$

The β parameter in Eq. (7) and in Table I is for diatomic A_2 in each case; this enables direct comparisons of the expressions for different sized clusters. Further, the angular momentum **J** is taken as dimensionless (as a multiple of $\hbar$) throughout this entire section and considered classically, so that **J** may be aligned with a principal rotation axis of the molecule. If desired the quantity $\mathbf{J}^2$ may be equated to the quantum number expression $J(J+1)$. In the remainder of this section we present the corresponding expressions for several cases not representable in terms of a single structural parameter.

For A_3 with $\mathbf{J}\perp C_3$ and C_2 (the J_y case) the actual molecular symmetry is C_{2v}, with two edges extended and one (parallel to **J**) slightly compressed, thus forming an acute isosceles triangle. We designate the two structural parameters as $z=(1+x)^{-2}$ and $Z=(1+X)^{-2}$, respectively, where x and X are the corresponding reduced displacements. The dispersion relations may be expressed parametrically in terms of these two variables as follows:

$$\beta J_y^2=16z^4(1-z^3)\left(\frac{1}{z}-\frac{1}{4Z}\right)^2, \tag{9}$$

$$0=z^4(1-z^3)+2Z^4(1-Z^3), \tag{10}$$

$$\epsilon=12z^4(1-z^3)\left(\frac{1}{z}-\frac{1}{4Z}\right)+2(1-z^3)^2+(1-Z^3)^2. \tag{11}$$

Because of the interdependence in Eq. (10) of the parameters, the energy depends in effect on a single variable.

For A_6 with $\mathbf{J}\parallel C_3$ the actual molecular symmetry is D_{3d}, with the 12 edges being comprised of two sets of 6, described by the parameters z for the six edges within the two triads whose planes are $\perp$ to **J** (C_3) and ζ for the six edges connecting these two triads, and the three *trans* distances being equal and described by the parameter Z, with the moment of inertia depending only upon z. The rotational energy dispersion, including these latter interactions, is represented by the following:

$$\beta J^2=144z^2(1-z^3)+72(Z^4/z^2)(1-Z^3), \tag{12}$$

$$0=36\zeta^2(1-\zeta^3)+18(Z^4/\zeta^2)(1-Z^3), \tag{13}$$

$$Z=z\zeta/(z+\zeta), \tag{14}$$

$$\epsilon=\beta J^2z/4+6(1-z^3)^2+6(1-\zeta^3)^2+3(1-Z^3)^2. \tag{15}$$

Note that Eqs. (13) and (14) give the interdependencies of the structural parameters, so that the energy again is in effect a function of a single parameter. The effective energy in Eq. (15) has a value of (588/257) for $J=0$, for which $z_0=\zeta_0=(264/257)^{1/3}$ and $Z_0=z_0/2$. The value $z_0=(264/257)^{1/3}=1.009\,00$ describes the compression ($x_0=-0.004\,47$) of the 12 edges due to the attractive *trans* interactions. The energy value (588/257) is relative to that for the unattainable structure with all 15 interacting pairs being at r_e ($z=\zeta=1$). It is desirable for some purposes to subtract this constant from the energy so that the energy is zero for $J=0$. We follow this latter convention in our energy tabulations and all discussion. Alternatively, relative to dissociated atoms the energy at $J=0$ is $(588/257)-15$, or -12.71206. Note also that β in Eqs. (12) and (15) is the value for diatomic A_2, so that rigid-rotor energy is given by $\beta J^2z_0/4$.

Again for the A_6 cluster but with $\mathbf{J}\| C_4$, so that the actual symmetry is D_{4h}, there are four edges in the equatorial plane described by the parameter z, eight edges by the parameter ζ, two *trans* distances in the equatorial plane described by $z/2$, and the unique *trans* distance, that parallel to $\mathbf{J}$, described by Z. The moment of inertia, as for the case of $\mathbf{J}\| C_3$, depends only upon z. The rotational energy dispersion is represented by the following:

$$\beta J^2 = 96z^2(1-z^3)+24(z/2)^2(1-(z/2)^3)-48(Z^4/z^2) \times(1-Z^3), \tag{16}$$

$$0=48\zeta^2(1-\zeta^3)+24(Z^4/\zeta^2)(1-Z^3), \tag{17}$$

$$Z=z\zeta/(2(2z-\zeta)), \tag{18}$$

$$\epsilon=\beta J^2 z/4+4(1-z^3)^2+8(1-\zeta^3)^2+2(1-(z/2)^3)^2 +(1-Z^3)^2. \tag{19}$$

Through the parameter interdependencies the energy is a function of a single variable.

V. ANGULAR MOMENTUM-CONSERVING SIMULATIONS

As a complement to our derivations of analytic rotational energy dispersions parametric in centrifugal displacements, we have written and utilized a C-language program for carrying out classical mechanical simulations on LJO clusters A_n with the imposed constraint of a fixed rotational angular momentum in the molecular frame. The procedure may be outlined as follows:

(1) A set of masses $\{m_i\}$ and initial coordinates $\{\mathbf{r}_i\}$ are selected with the center of mass of the cluster at the origin.

(2) A magnitude and direction for the angular momentum $\mathbf{J}$ with respect to the molecular frame is selected. Typically this direction corresponds to a principal axis of the moment of inertia tensor $\mathbf{I}$.

(3) The moment of inertia tensor $\mathbf{I}$ is calculated from the masses and coordinates. The angular velocity $\boldsymbol{\omega}$ is calculated from inversion of the relationship $\mathbf{J}=\mathbf{I}\boldsymbol{\omega}$, that is, from $\boldsymbol{\omega}=\mathbf{I}^{-1}\mathbf{J}$.

(4) The vector force $\mathbf{F}_i^r$ acting on the ith particle due to rotation is calculated as

$$\mathbf{F}_i^r=-m_i[\boldsymbol{\omega}\times(\boldsymbol{\omega}\times\mathbf{r}_i)].$$

To this force is added the force $\mathbf{F}_i^{\rm el}$ arising from the pairwise-additive LJO potential energy $\epsilon_{\rm el}$, that is,

$$\mathbf{F}_i^{\rm el}=-\nabla_i\epsilon_{\rm el}.$$

(5) The system is assumed to evolve toward a minimum energy configuration, subject to the constraint of fixed $\mathbf{J}$. That is, a time step is assumed and a set of displacements calculated from the set of total forces $\{\mathbf{F}_i\}=\{\mathbf{F}_i^r+\mathbf{F}_i^{\rm el}\}$. The process is repeated starting from the new set of coordinates, ignoring the acquired velocities (equivalent to setting the kinetic energy, other than the rotational kinetic energy associated with $\mathbf{J}$, equal to zero), until the total energy has converged to a change not exceeding 10^{-8} ppb from the previous iteration [in practice separate convergence for the rotational kinetic energy and the (vibrational) potential energy is required].

The time step in (5) is typically taken as 0.1 ps, with convergence typically achieved in about 100 to 1000 iterations, or 10 to 100 ps. If a series of increasing magnitudes of $\mathbf{J}$, all with the same direction in the molecular frame, are to be considered, the optimized geometry from one run is used as the initial geometry for the next, thus reducing the number of steps required for convergence. Occasionally several thousand iterations are required, especially when major geometrical changes accompany small increases in the magnitude of $\mathbf{J}$. An example discussed later is the collapse of the tetrahedral structure of A_4 with $\mathbf{J}\| S_4$ to a square-planar structure with $\mathbf{J}\| C_4$ at a sufficiently high angular momentum.

The procedure outlined above closely resembles that employed by Li and Jellinek[13] in their simulation studies of rotational distortion, isomerization, and fragmentation of the Ar_{13} cluster. Their procedure, which was based on their earlier demonstration that overall rotation can be separated from vibrational (internal) motion in any N-body system, however floppy, incorporated the quenching of the "thermal" energy every 2.5 ps as the system undergoes its Hamiltonian evolution. Our procedure is somewhat simpler in that no equations of motion are actually solved; only a quasivelocity vector for each particle is calculated as the total force divided by the mass and multiplied by a time increment, with all velocities reset to zero at the end of each step (the rotation of the reference frame is ignored).

In every case considered the energies and structures obtained using the simulation program agree with those obtained using our analytic rotational energy dispersions parametric in centrifugal displacements, so that each procedure serves as a check on the other. What may be called exceptions to this agreement are the cases where the assumption of a particular molecular symmetry in the choice of analytic expressions, while correctly describing that case, fails to predict the existence of lower energy structures. The collapse of tetrahedral A_4 to square-planar A_4 mentioned above was "discovered" in our simulations and then after-the-fact confirmed by comparing the analytic expressions for the two cases.

VI. RESULTS AND DISCUSSION

A. Reduced spectroscopic constants

We present in Table II a compilation of dimensionless reduced quadratic, quartic, and sextic constants for the LJO clusters A_n together with values in cm^{-1} for the specific cases of Ar_n. The quadratic constants are simply the respective rigid rotor expressions, namely βJ^2 for A_2 and for A_3 with $\mathbf{J}\perp C_3$, $\beta J^2/2$ for A_3 with $\mathbf{J}\| C_3$ and for A_4, and $\beta J^2 z_0/4$ with $z_0=(264/257)^{1/3}$ for A_6, where $\beta=\beta(A_2)$. We obtain the higher coefficients from limits as $J\to 0$ of expressions written in terms of displacements as shown below. Let the reduced energy (in units of the diatomic well depth) be written as

$$\epsilon=\epsilon_0-\delta J^4+hJ^6+\cdots, \tag{20}$$

TABLE II. Summary of quadratic, quartic, and sextic coefficients for clusters A_n ($n=2-6$).

Molecule	Direction	Symmetry	β[a]	$B(\mathrm{Ar}_n)$[b]	δ[c]	$D(\mathrm{Ar}_n)$[b]	h[d]	$H(\mathrm{Ar}_n)$[b]
A_2	J⊥ C_∞	$D_{\infty h}$	1	0.058	1	1.11×10^{-6}	−1	-8.44×10^{-11}
A_3	J‖ C_2	C_{2v}	1	0.058	1	1.11×10^{-6}	−1	-8.44×10^{-11}
	J⊥ C_2	C_{2v}	1	0.058	1	1.11×10^{-6}	−1/9	-9.38×10^{-12}
	J‖ C_3	D_{3h}	1/2	0.029	1/12	9.21×10^{-8}	−1/72	-1.17×10^{-12}
A_4	J‖ C_3	C_{3v}	1/2	0.029	1/12	9.21×10^{-8}	−1/32	-2.64×10^{-12}
	J‖ S_4	D_{2d}	1/2	0.029	1/8	1.39×10^{-7}	−1/72	-1.17×10^{-12}
	Scalar[e]	···	···	···	1/10	1.11×10^{-7}	···	···
	Tensor[f]	···	···	···	1/160	6.94×10^{-9}	···	···
A_6	J‖ C_3	D_{3d}	$z_0/4$[g]	0.015	0.00987[h]	1.10×10^{-8}	···	···
	J‖ C_4	D_{4h}	$z_0/4$	0.015	0.01605[h]	1.78×10^{-8}	···	···
	Scalar[e]	···	···	···	0.01234[h]	1.37×10^{-8}	···	···
	Tensor[f]	···	···	···	0.00093[h]	1.03×10^{-9}	···	···

[a]Reduced values B/d in units of $\beta(\mathrm{Ar}_2)=\hbar^2/2\mu r_e^2 d$.
[b]Values in cm^{-1} for Ar_n based on $\beta(\mathrm{Ar}_2)=6.878\times10^{-4}$ and $d=84.1\ \mathrm{cm}^{-1}$.
[c]Reduced values D/d in units of $\beta^2/36$ with $\beta=\beta(A_2)$.
[d]Reduced values H/d in units of $\beta^3/324$ with $\beta=\beta(A_2)$.
[e]Scalar values δ_s given by $(3\delta_3+2\delta_4)/5$ with $\delta_i=36[(\epsilon_0-\epsilon_i)/\beta^2J^4]$, $i=3$ or 4, with rigid-rotor energies $\epsilon_0=(\beta J^2/2)$ for A_4 and $(\beta J^2/4)(264/257)^{1/3}$ for A_6.
[f]Tensor values δ_t given by $3(\delta_4-\delta_3)/20$.
[g]$z_0=(264/257)^{1/3}$.
[h]The limits are as follows: $\delta_3=(35\ 25\ 043\ 519/23\ 357\ 949\ 542\ 400)33^{2/3}257^{1/3}$ and $\delta_4=(12\ 323/50\ 207\ 256)33^{2/3}257^{1/3}$, with δ_s and δ_t given by footnotes e and f.

where ϵ_0 is the rigid rotor energy expressed as a function of the displacement related variable z (or a set of z_i's). *By this we mean that the energy of a rigid rotor as a function of angular momentum* **J** *is written parametrically as a function of the displacement suffered by the corresponding nonrigid rotor with the same* **J** (the rigid rotor by definition suffers no displacement). Thus

$$\left(\frac{\delta}{\beta^2}\right)=\lim_{\epsilon_0\to0}\left(\frac{\epsilon_0-\epsilon}{\epsilon_0^2}\right), \tag{21}$$

$$\left(\frac{h}{\beta^3}\right)=-\lim_{\epsilon_0\to0}\left(\frac{\epsilon_0-\delta J^4-\epsilon}{\epsilon_0^3}\right). \tag{22}$$

Higher coefficients may similarly be extracted from the dispersion relations if desired. All quantities appearing on the right side of the above equations are expressed in terms of displacements, not J. We have obtained these limits analytically, checking them against numerical limits as $J\to0$ obtained using the simulation program described in Sec. V. Specific cases are discussed below.

B. The equilateral triangular cluster A_3

In Table III we present the reduced energies ϵ as a function of βJ^2 for three cases for A_3, namely J‖ $C_2(J_x)$, J⊥ $C_2(J_y)$, and J‖ $C_3(J_z)$, as based on the expressions in Table I and on Eqs. (9)–(11). Also listed is the (rounded-off) quantum number J for each value of βJ^2 for the particular case of Ar_3. We note that the ratio ϵ_x/ϵ_y, identically equal to unity for a rigid symmetric top, falls to 0.977 38 at

TABLE III. Centrifugal energies[a,b] for $A_3(D_{3h})$.

ϵ_x	ϵ_y	ϵ_z	ϵ_x/ϵ_y	$2\epsilon_z/\epsilon_y$	βJ^2	$J(\mathrm{Ar}_3)$[c]
0	0	0	(1.0)	(1.0)	0	0
0.742 49	0.743 87	0.378 72	0.998 14	1.018 24	0.760 16	33
1.162 22	1.168 58	0.601 75	0.994 56	1.029 88	1.210 44	42
1.521 84	1.539 81	0.801 55	0.988 33	1.041 10	1.615 56	48
1.800 00[d]	1.841 66	0.968 00	0.977 38	1.051 22	1.954 38	53
(1.665 78)[e]	2.562 36	1.385 03	···	1.081 03	2.808 69	64
(1.772 28)	2.899 69	1.595 61	···	1.100 54	3.243 21	69
(1.844 87)	3.110 50[f]	1.738 96	···	1.118 12	3.540 29	72
(2.110 53)	···	2.262 12	···	···	4.633 89	82
(2.888 47)	···	3.776 38	···	···	7.902 36	107
(3.381 36)	···	4.712 26	···	···	10.036 61	121
(3.761 18)	···	5.400 00[d]	···	···	11.726 28	130

[a]Subscripts x, y, and z denote J‖ $C_2(J_x)$, J⊥ $C_2(J_y)$, and J‖ $C_3(J_z)$, respectively.
[b]All energies in units of diatomic A_2 well depth.
[c]Based on $\beta(\mathrm{Ar}_2)=6.878\times10^{-4}$.
[d]Displacement = 0.164 99.
[e]Energies in parentheses are for collinear structures. For $J=0$ this structure has an energy of 2646/2731.
[f]Displacement = 0.190 98; edge ‖ to **J** undergoes compressive displacement = −0.011 68.

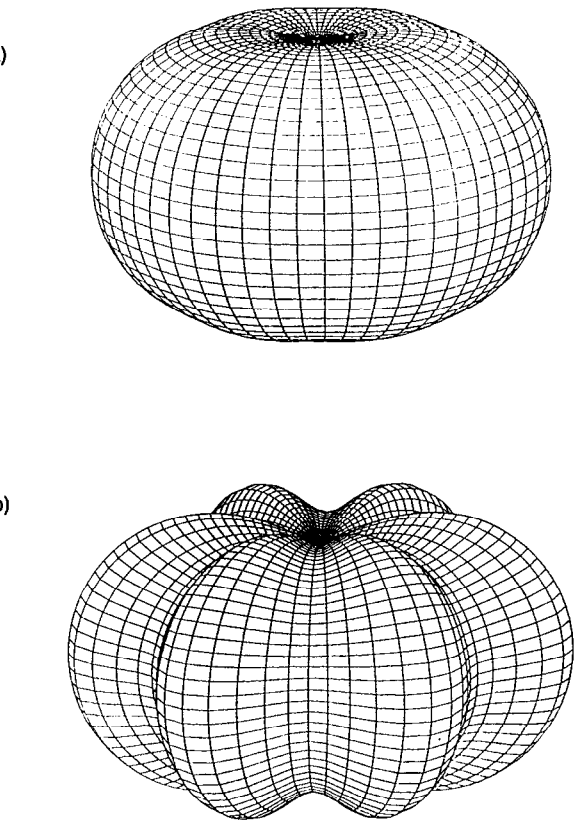

FIG. 1. Rotational energy surface for the LJO cluster A_3 (see Sec. VI B for definition). While the (undistorted) molecular symmetry is D_{3h}, that for the surface is D_{6h}. The upper figure (a) is to scale based on energies of 1.8, 1.841 66, and 0.968 00 (units of diatomic A_2 dissociation energy) for J_x, J_y, and J_z, respectively [$\beta J^2=9(2/5)^{5/3}=1.954\ 38$, corresponding to $J=53$ for Ar_3] and is obtained by interpolations assuming $\cos(6\phi)$ and $\cos(2\theta)$ dependencies. The lower figure (b) is similar, but with the ϕ angular variation greatly exaggerated for emphasis by taking the J_y energy to be 2.0 units rather than 1.841 66.

the maximum of $\epsilon_x=9/5$. Similarly the ratio $2\epsilon_z/\epsilon_y$ rises from unity to a value of 1.118 12 at the maximum for ϵ_y. These deviations from unity reflect the nonrigidity of the A_3 rotor. In Fig. 1(a) we show the rotational energy surface in **J** space, that is, the variation of the energy ϵ with respect to the direction of **J** in the molecular frame for some fixed magnitude of **J**. The surface is not cylindrically symmetrical as it would be for a rigid symmetric top, but rather possesses sixfold rotational symmetry (there are three C_2 axes, with clockwise and counterclockwise rotations about each having the same energy, hence there are six equivalent directions in **J** space). This figure is constructed from J_x, J_y, and J_z energies of 1.8, 1.841 66, and 0.968 00 for $\beta J^2=9(2/5)^{5/3}=1.954\ 38$ by an interpolation assuming $\cos(6\phi)$ and $\cos(2\theta)$ angular dependencies. Figure 1(b) is similar, but with the ϕ angular variation greatly exaggerated by taking the J_y energy to be 2.0 units rather than 1.841 66. A better plotting procedure, illustrated in the $\{J_x,J_z\}$ plane containing the C_3 axis, would be to construct $\beta J^2=f(z_x,z_z)$ and $\epsilon=g(z_x,z_z)$, select βJ^2 and z_x, say, and solve for z_z and ϵ. As an example, with $\beta J^2=1.954\ 38$ and $z_x=0.92$, $z_z=0.992\ 13$ and $\epsilon=1.496\ 59$, while a $\cos(2\theta)$ interpolation ($\theta=49.3°$) yields $\epsilon=1.446\ 46$, an error of 3.5% which is insignificant for graphical purposes (the percentage error is less for smaller values of βJ^2). We further note that past the energy maximum of 9/5 for the J_x case that the preferred structure is actually collinear; the triangular molecule "snaps" open! (For $J=0$ the collinear $D_{\infty h}$ structure has an energy of $2646/2731=0.968\ 88$ relative to that for the D_{3h} structure.) We note here that the description of molecular rotation as corresponding to the J_x, J_y, or J_z cases is classical; semiclassically the J_x case defines a separatrix, with **J** for energies greater than that for J_x executing a closed path about one of the twofold axes (there a six symmetry equivalent such possibilities on this D_{3h} rotational energy surfacc) but with **J** for energies less than that for J_x executing an undulating path about the C_3 axis (the projection on the J_z axis is not constant). The concomitant semiclassical centrifugal distortions may be described as distortion waves formed from the static distortions described above. Finally the question of symmetry breaking in A_3 with $\mathbf{J}\|\ C_3$ is discussed in Sec. VII.

In Table II we present the reduced quartic and sextic coefficients for A_3; the corresponding values for diatomic A_2 are included for reference. As expressed in reduced units the diatomic value of δ for A_2 is $\beta^2/36$; the $J=0$ limiting values for A_3 are the fractions 1, 1, and 1/12 of this diatomic value for the J_x, J_y, and J_z cases, respectively. The fact that the values are the same for the J_x and J_y cases indicates that the energy differences between these two cases as shown by the rotational energy surface are associated with a higher-order term, namely sextic (J^6), in a power series expansion, corresponding to the six-fold symmetry described above. Indeed the reduced sextic coefficients h are 1, 1/9, and 1/72 times the diatomic value of $-\beta^3/324$ for the J_x, J_y, and J_z cases, respectively. Thus the smaller magnitude of the negative h value for the $J_y(\mathbf{J}\perp\ C_2)$ case as compared to the $J_x(\mathbf{J}\|\ C_2)$ case corresponds to the higher energy for the former as compared to the latter for the same magnitude of **J**.

C. The tetrahedral cluster A_4

In Table IV we similarly present numerical results for the tetrahedral cluster A_4. The two cases are for $\mathbf{J}\|\ C_3(C_{3v})$ and $\mathbf{J}\|\ S_4(D_{2d})$. The striking result is that the latter is energetically preferred for a given angular momentum, that is, this deformable spherical top will make itself into a symmetric top with a preferred S_4 axis. The reduced δ values in Table II have $J=0$ limits of 1/12 and 1/8 in units of the corresponding value for diatomic A_2; these may be converted (Ref. 1) to the "spherical" and "cubic" tensor coefficients δ_s and δ_t as shown. The latter has a limiting value of 1/160 in units of the diatomic δ. Although small, this coefficient is the critical measure of the nonspherical effects of centrifugal distortion and is a measure of the associated splittings of the rigid spherical top rotational energy levels. Finally we note for A_4 that the square-planar structure, unstable for zero or low angular momentum with respect to an out-of-plane puckering leading to a tetrahedral structure (for $J=0$ the D_{4h} structure

TABLE IV. Centrifugal displacements[a] and energies[a,b] for $A_4(T_d)$.

x_3	ϵ_3	x_4	ϵ_4	ϵ_4/ϵ_3	βJ^2	$J(\mathrm{Ar}_4)$[c]
0	0	0	0	(1.0)	0	0
0.010 15	1.006 44	0.015 88	1.001 13	0.994 72	2.032 78	54
0.020 62	1.875 46	0.034 09	1.854 48	0.988 81	3.824 18	75
0.031 42	2.618 96	0.056 12	2.571 85	0.982 01	5.389 06	88
0.042 57	3.248 93	0.086 21	3.163 74	0.973 78	6.743 46	99
0.053 17	3.738 20	0.164 99	3.600 00	0.963 03	7.817 52	107
0.084 65	4.712 26	···	(4.029 78)[d]	···	10.036 60	121
0.118 03	5.211 84	···	(4.325 30)	···	11.243 52	128
0.164 99	5.400 00	···	(4.443 10)	···	11.726 30	131

[a]Subscripts 3 and 4 denote $\mathbf{J}\|\ C_3(C_{3v})$ and $\mathbf{J}\|\ S_4(D_{2d})$, respectively.
[b]All energies in units of diatomic A_2 well depth.
[c]Based on $\beta(\mathrm{Ar}_2)=6.878\times10^{-4}$.
[d]Energies in parentheses represent structures which have collapsed to D_{4h}. For $J=0$ this structure has an energy of 25 284/16 641 = 1.519 38.

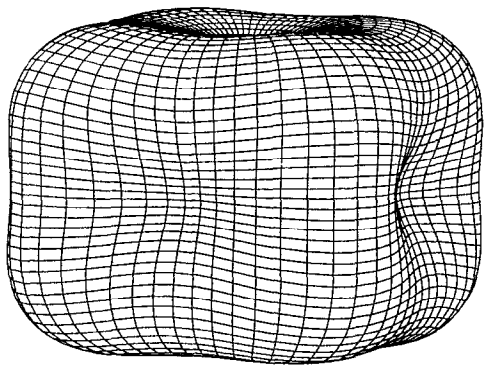

FIG. 2. Rotational energy surface (qualitative shape) for the LJO clusters A_4 and A_6. The symmetry of the surface is O_h, with eight energy maxima for $\mathbf{J}\|\ C_3$ and six energy minima for $\mathbf{J}\|\ S_4(A_4)$ or $C_4(A_6)$.

has an energy of 25 284/16 641 = 1.519 38 relative to that for the T_d structure), actually becomes the stable form past the energy maximum of 18/5 for the $\mathbf{J}\|\ S_4$ case; this behavior, in which the tetrahedron "collapses" into a plane, is similar to that described above for A_3 becoming linear past the energy maximum of 9/5 for the J_x case.

D. The octahedral cluster A_6

The octahedral cluster A_6 differs from the preceding in that there is no arrangement permitting all interacting pairs to be at the diatomic equilibrium separation r_e. The resulting "compression" of the octahedron was discussed in Sec. IV. Reduced energies are given in Table V for three cases, namely $\mathbf{J}\|\ C_3(D_{3d})$, $\mathbf{J}\|\ C_2(D_{2h})$, and $\mathbf{J}\|\ C_4(D_{4h})$. All interactions, including the three *trans* interactions, are included in each case. As with tetrahedral A_4, the case with $\mathbf{J}\|\ C_3$ is highest in energy, thus corresponding to eight energy maxima on the rotational energy surface (Fig. 2). This result is surprising, as the molecules CH_4 (tetrahedral) and SF_6 (octahedral) are known to have opposite behaviors; the $\mathbf{J}\|\ C_3$ case corresponds to rotational energy maxima for CH_4 but minima for SF_6. Thus the reduced quartic coefficient δ_t for A_6 in Table II has the same sign as that for A_4, although the magnitude is a factor of eight smaller.

TABLE V. Centrifugal energies[a,b] for $A_6(O_h)$.

ϵ_3	ϵ_2	ϵ_4	ϵ_4/ϵ_3	βJ^2	$J(\mathrm{Ar}_6)$[c]
0	0	0	(1.0)	0	0
0.072 84	0.072 84	0.072 83	0.999 86	0.288 86	20
0.284 17	0.284 12	0.283 95	0.999 23	1.127 94	40
0.633 21	0.632 96	0.632 08	0.998 21	2.517 24	60
1.118 66	1.117 93	1.115 00	0.996 73	4.456 75	80
1.738 61	1.737 00	1.729 35	0.994 67	6.946 48	100
2.490 48	2.487 58	2.470 25	0.991 88	9.986 42	120
3.370 89	3.366 46	3.330 59	0.988 04	13.576 58	140
4.375 48	4.369 80	4.299 14	0.982 55	17.716 96	160
5.498 55	5.492 98	5.352 07	0.973 36	22.407 55	180

[a]Subscripts 2, 3, and 4 denote $\mathbf{J}\|\ C_2(D_{2h})$, $\mathbf{J}\|\ C_3(D_{3d})$, and $\mathbf{J}\|\ C_4(D_{4h})$, respectively.
[b]All energies in units of diatomic A_2 well depth with the energy for $J=0$ being $-12.712\,06$ relative to dissociation to form 6 A.
[c]Based on $\beta(\mathrm{Ar}_2)=6.878\times10^{-4}$.

VII. SYMMETRY BREAKING FOR $A_3(D_{3h})$ WITH $\mathbf{J}\|\ C_3$

An interesting and important question is the following: Is it possible for a molecule to suffer a spontaneous lowering of its symmetry at some sufficiently high rotational angular momentum? Stated differently, can a cluster having a stable configuration at low angular momentum as characterized by all-real vibrational frequencies (all-positive eigenvalues of the hessian matrix) become at high angular momentum unstable as characterized at least one imaginary vibrational frequency (at least one negative eigenvalue of the hessian matrix)? We explore this question here with the example of the cluster A_3 with $\mathbf{J}\|\ C_3$, for which there is the possibility of a symmetry lowering to C_{2v} or even to C_s at some critically high value of the angular momentum. To do this we must obtain the hessian, or second-derivative, matrix in coordinate space (not $\mathbf{J}$ space), so first we rewrite the reduced energy ϵ in terms of the individual displacement-related variables $z_i \equiv (1+x_i)^{-2}$ as follows:

$$\epsilon=\epsilon_r+\epsilon_{\mathrm{el}}=\frac{3\beta J^2}{2\Sigma_{i=1}^{3} z_i^{-1}}+\sum_{i=1}^{3}(1-z_i^3)^2, \tag{23}$$

where $\beta=\beta(A_2)=2\beta(A_3)$. We define a reduced hessian as the matrix with elements $\{\partial^2\epsilon/\partial x_i\,\partial x_j\}$; the hessian $\mathbf{h}$ can conveniently be expressed in terms of the $\{z_i\}$ as follows:

$$h_{ii}=\frac{3\beta J^2(3z_i^{-1}-\Sigma_{j\neq i} z_j^{-1})}{\Sigma_{k=1}^{3} z_k^{-1}}+12z_i^4(13z_i^3-7), \tag{24}$$

$$h_{ij}=\frac{12\beta J^2 z_i^{-1/2} z_j^{-1/2}}{\Sigma_{k=1}^{3} z_k^{-1}}, \quad i\neq j. \tag{25}$$

Note that the contribution to the hessian from ϵ_{el} is diagonal. If evaluated for a D_{3h} structure, for which each $z_i=z$, the hessian reduces to

$$\mathbf{h}=\frac{\beta J^2 z^2}{9}\begin{pmatrix}1&4&4\\4&1&4\\4&4&1\end{pmatrix}+12z^4(13z^3-7)\begin{pmatrix}1&0&0\\0&1&0\\0&0&1\end{pmatrix}. \tag{26}$$

The eigenvalues of the rotational part of the hessian are -3, -3, and 9, in units of $\beta J^2 z^2/9$; these values add to $12z^4(13z^3-7)$ to give the eigenvalues of the total hessian. This addition is valid because the "electronic" part of the hessian is not only diagonal but is proportional to a unit matrix. The same formalism applies to other pairwise-additive potential energy expressions such as those for pairwise-additive harmonic (HO) or Morse (MO) oscillators; the LJO contribution of $12z^4(13z^3-7)$ is simply replaced by the appropriate form, namely the force constant k in the HO case. For the LJO case the onset of rotational instability is found by setting the doubly degenerate eigenvalue equal to zero and by requiring that the pathway condition $\beta J^2=f(z)$ be satisfied. That is, the onset is given by the solution of

$$\beta J^2=36z^2(13z^3-7)=36z^2(1-z^3), \tag{27}$$

where β again is for the reference diatomic A_2. The solution is $z^3=4/7$, corresponding to a reduced displacement of $x=(7/4)^{1/6}-1=0.097\,76$, for which the reduced energy ϵ is $243/49=4.959\,18$ relative to the well minimum, or $96/49=1.959\,18$ above dissociation to form $3A$. This energy is approximately half a unit below the maximum value of $\epsilon=27/5=5.4$ for effective energies with $\mathbf{J}\|\ C_3$ which occurs at $z^3=2/5$, corresponding to $x=(5/2)^{1/6}-1=0.164\,99$. Using $\beta(\mathrm{Ar}_2)=6.878\times10^{-4}$, the onset of such instability occurs near $J=124$ for the cluster Ar_3. Thus we conclude that rotational instability, in the sense of there being at least one imaginary J-dependent vibrational mode,[14,15] can occur for this example, but only at very high angular momenta. We note that the energy of 243/49 at the onset of instability has contributions of $216/49=4.408\,16$ from rotation and $27/49=0.551\,02$ from the potential energy of bond stretching. Finally we note that while similar solutions may be found for the pairwise-additive MO system, no solutions exist for the pairwise-additive HO system.

VIII. SUMMARY

We have studied by means of both analytic derivations and simulations the rotational energy dispersions of small van der Waals clusters bound by pairwise Lennard-Jones interactions; these clusters model those formed from rare-gas atoms or other closed-shell moieties. Some further details of these results have been published elsewhere.[33] While our present analysis has ignored vibration, our earlier study[6] did include a harmonic oscillator (HO) approximation to the zero-point energy (ZPE) for the LJO diatomic A_2. This correction was based on the reduced force constant $k=(\partial^2\epsilon/\partial x^2)=24z^4(5z^3-2)$, which equals 72 for $J=0$ ($z=1$) and which decreases with increasing J. We showed that inclusion of the associated ZPE reduced the error in the quartic coefficient δ from 5.3% to 0.2% as compared to the exact quantum mechanical value[34] for $\beta=10^{-4}$, with similar improvement being obtained for higher coefficients. In a future study we shall present a treatment of the J-dependent vibrations of small LJO clusters. Our present dispersions, which represent the variation of the energies of the deformable molecules with respect to the magnitude and direction of their rotational angular momenta, are typically represented analytically by sets of equations parametric in centrifugal displacement coordinates. Our specific results include quartic and sextic spectroscopic constants obtained analytically from the rotational energy dispersion relationships for the clusters A_3, A_4, and A_6. Results are expressed in reduced, dimensionless units and are thus applicable to a wide range of systems, although specific application is made to argon clusters.

A striking result is that for both A_4 and A_6 the sign of the cubic anisotropy in the dispersions is such that these nominally spherical tops each display a preference for the rotational angular momentum to be along a fourfold rotation axis, with angular momentum along a threefold axis representing a rotational energy maximum (Fig. 2). It is instructive to compare the computed values of the quartic tensor coefficient $D_t=d\delta_t$ for Ar_4 and Ar_6 as given in Table II to those observed for other spherical tops. Both the Ar_4 value of 6.94×10^{-9} cm^{-1} and the Ar_6 value of 1.03×10^{-9} cm^{-1} are much smaller than that observed[35] for CH_4 of $(4.434\,515\pm0.000\,123)\times10^{-6}$ cm^{-1}. However both are larger in magnitude, and opposite in sign, to the value observed[36] for SF_6 of $-(1.863\,83\pm0.000\,65)\times10^{-10}$ cm^{-1}. For SF_6 the consequence of D_t being negative is that for a given J, say 30, there is found in the computed energy-level spectrum[37,38] a lowest-energy cluster of eight states associated with the projection $K_3=30$ (on a threefold axis) and having a degeneracy pattern 1:3:3:1 and a highest-energy cluster of six states associated with the projection $K_4=30$ (on a fourfold axis) and having a degeneracy pattern 1:3:2. The total frequency spread for the SF_6 $J=30$ manifold of states is approximately 27 MHz, with the spread within the K_3 cluster being 30 kHz. For Ar_4 and Ar_6 the pattern will be inverted as compared to SF_6 and will have spacings approximately 38 and 6 times larger, respectively. The difference in the sign of D_t between SF_6 and CH_4 can be attributed to the different directionalities of the bonds, with D_{4h} structures ($\mathbf{J}\|\ C_4$) for SF_6 lying higher in energy than D_{3d} structures ($\mathbf{J}\|\ C_3$) with the same J as the former involves bond stretching only while the latter involves bond bending as well. The strongest interactions within the clusters A_4 and A_6 are along the edges; A_4 is similar to A_6 in that the primary centrifugal distortion is the stretching of the edges in the plane normal to J, these edges being 2 in number for A_4 with $\mathbf{J}\|\ S_4$ but 3 for $\mathbf{J}\|\ C_3$, and 4 in number for A_6 with $\mathbf{J}\|\ C_4$ but 6 for $\mathbf{J}\|\ C_3$. It is this ratio of 2 to 3 for both A_4 and A_6 which accounts for their having the same sign of δ_t, with the particular sign corresponding to lower energies for the structures involving the fewer edge stretchings.

ACKNOWLEDGMENTS

We gratefully acknowledge very helpful discussions held with J. Hougen (NIST), J. Jellinek (Argonne National Laboratory), and G. Natanson (Computer Science Corporation).

[1] L. L. Lohr and J.-M. J. Popa, J. Chem. Phys. **84**, 4196 (1986).
[2] L. L. Lohr and A. J. Helman, J. Comput. Chem. **8**, 307 (1987).
[3] L. L. Lohr, Int. J. Quantum Chem. Quantum Symp. Symp. **21**, 407 (1987).
[4] A. Taleb-Bendiab and L. L. Lohr, J. Mol. Spectrosc. **132**, 413 (1988).
[5] L. L. Lohr, J. Mol. Struct. (THEOCHEM) **199**, 265 (1989).
[6] L. L. Lohr, J. Mol. Spectrosc. **155**, 205 (1992).
[7] R. S. Berry, J. Jellinek, and G. Natanson, Chem. Phys. Lett. **107**, 227 (1984).
[8] R. S. Berry, J. Jellinek, and G. Natanson, Phys. Rev. A **30**, 919 (1984).
[9] J. Jellinek, T. L. Beck, and R. S. Berry, J. Chem. Phys. **84**, 278 (1986).
[10] R. S. Berry, T. L. Beck, H. L. Davis, and J. Jellinek, Adv. Chem. Phys. **70** (part 2), 75 (1988).
[11] N. Quirke, Molecular Simulations **1**, 249 (1988).
[12] D. M. Leitner, R. M. Whitnell, and R. S. Berry, J. Chem. Phys. **91**, 3470 (1989).
[13] D. H. Li and J. Jellinek, Z. Phys. D **12**, 177 (1989).
[14] J. Jellinek and D. H. Li, Phys. Rev. Lett. **62**, 241 (1989).
[15] J. Jellinek and D. H. Li, Chem. Phys. Lett. **169**, 380 (1990).
[16] T. R. Horn, R. B. Gerber, J. J. Valentini, and M. A. Ratner, J. Chem. Phys. **94**, 6728 (1991).
[17] H. Cheng and R. S. Berry, Phys. Rev. B **45**, 7969 (1992).
[18] D. M. Leitner, J. D. Doll, and R. M. Whitnell, J. Chem. Phys. **96**, 9239 (1992).
[19] C. D. Maranas and C. A. Floudas, J. Chem. Phys. **97**, 7667 (1992).
[20] C. A. Parish and C. E. Dykstra, J. Chem. Phys. **98**, 437 (1993).
[21] A. R. Cooper, S. Jain, and J. M. Hutson, J. Chem. Phys. **98**, 2160 (1993).
[22] X. Hu and W. L. Hase, J. Phys. Chem. **96**, 7535 (1992).
[23] W. J. Chesnavich, J. Chem. Phys. **77**, 2988 (1982).
[24] K. Rynefors and S. Nordholm, Chem. Phys. **95**, 345 (1985).
[25] E. Pollak, J. Chem. Phys. **86**, 1645 (1987).
[26] M. Berblinger, J. M. Gomez-Llorente, E. Pollak, and Ch. Schlier, Chem. Phys. Lett. **146**, 353 (1988).
[27] M. Berblinger, E. Pollak, and Ch. Schlier, J. Chem. Phys. **88**, 5643 (1988).
[28] R. A. Aziz and H. H. Chen, J. Chem. Phys. **67**, 5719 (1977).
[29] E. Scoles, Annu. Rev. Phys. Chem. **31**, 81 (1980).
[30] M. J. Ondrechen, Z. Berkovitch-Yellin, and J. Jortner, J. Am. Chem. Soc. **103**, 6586 (1981).
[31] C. Douketis, G. Scoles, S. Marchetti, M. Zen, and A. L. Thakker, J. Chem. Phys. **76**, 305 (1982).
[32] R. A. Aziz and M. Salman, Mol. Phys. **58**, 679 (1986).
[33] L. L. Lohr and C. H. Huben, in *Mathematical Computation with Maple V: Ideas and Application. Proceedings of the Maple Summer Workshop and Symposium, 1993,* edited by T. Lee (Birkhäuser, Boston, 1993), pp. 137–143.
[34] J. Tellinghuisen, J. Mol. Spectrosc. **122**, 455 (1987).
[35] C. W. Holt, M. C. Gerry, and I. Ozier, Can. J. Phys. **53**, 1791 (1975).
[36] B. Bobin, C. J. Bordé, J. Bordé, and C. Bréant, J. Mol. Spectrosc. **121**, 91 (1987).
[37] K. Fox, H. W. Galbraith, B. J. Krohn, and J. D. Louck, Phys. Rev. A **15**, 1363 (1977).
[38] W. G. Harter, C. W. Patterson, and F. J. Paixao, Rev. Mod. Phys. **50**, 37 (1978).